

RESEARCH ARTICLE

Deoxyribonucleoside treatment rescues EtBr-induced mtDNA depletion in iPSC-derived neural stem cells with POLG mutations

Cecilie Katrin Kristiansen^{1,2}  | Jessica Furriol³  | Anbin Chen^{1,4}  |
Gareth John Sullivan^{5,6,7}  | Laurence A. Bindoff^{1,8,9}  | Kristina Xiao Liang^{1,2} 

¹Department of Clinical Medicine, University of Bergen, Bergen, Norway

²Neuro-SysMed, Center of Excellence for Clinical Research in Neurological Diseases, Haukeland University Hospital, Bergen, Norway

³Department of Medicine, Haukeland University Hospital, Bergen, Norway

⁴Department of Neurosurgery, Xinhua Hospital Affiliated with Shanghai Jiaotong University School of Medicine, Shanghai, China

⁵Department of Molecular Medicine, Institute of Basic Medical Sciences, University of Oslo, Oslo, Norway

⁶Institute of Immunology, Oslo University Hospital, Oslo, Norway

⁷Department of Pediatric Research, Oslo University Hospital, Oslo, Norway

⁸Department of Neurology, Haukeland University Hospital, Bergen, Norway

⁹National Advisory Unit for Congenital Metabolic Diseases, Oslo University Hospital, Oslo, Norway

Correspondence

Kristina Xiao Liang, Department of Clinical Medicine, University of Bergen, P. O. Box 7804, 5020 Bergen, Norway.

Email: xiao.liang@uib.no

Laurence A. Bindoff, Department of Neurology, Haukeland University Hospital, P. O. Box 7804, 5020 Bergen, Norway.

Email: laurence.bindoff@uib.no

Funding information

Gerda Meyer Nyquist Guldbrandson og Gerdt Meyer Nyquists legat, Grant/Award Number: 103816102; L. Meltzers Høyskolefond (Meltzerfondet), Grant/Award Number: 103517133; Norges

Abstract

Mutations in *POLG*, the gene encoding the catalytic subunit of the mitochondrial DNA (mtDNA) polymerase gamma (Pol- γ), lead to diseases driven by defective mtDNA maintenance. Despite being the most prevalent cause of mitochondrial disease, treatments for *POLG*-related disorders remain elusive. In this study, we used *POLG* patient-induced pluripotent stem cell (iPSC)-derived neural stem cells (iNSCs), one homozygous for the *POLG* mutation c.2243G>C and one compound heterozygous with c.2243G>C and c.1399G>A, and treated these iNSCs with ethidium bromide (EtBr) to study the rate of depletion and repopulation of mtDNA. In addition, we investigated the effect of deoxyribonucleoside (dNs) supplementation on mtDNA maintenance during EtBr treatment and post-treatment repopulation in the same cells. EtBr-induced mtDNA depletion occurred at a similar rate in both patient and control iNSCs, however, restoration of mtDNA levels was

Abbreviations: D0, day 0; dA, deoxyadenosine; dC, deoxycytidine; DEGs, differentially expressed genes; dG, deoxyguanosine; dNs, deoxyribonucleosides; dNTPs, deoxyribonucleotide triphosphates; DPBS^{-/-}, DPBS without calcium and magnesium; dT, deoxythymidine; EtBr, ethidium bromide; ICC, immunocytochemistry; iNSCs, iPSC-derived neural stem cells; iPSCs, induced pluripotent stem cells; MSCAE, mitochondrial spinocerebellar ataxia with epilepsy; mtDNA, mitochondrial DNA; PEO, progressive external ophthalmoplegia; Pol- γ , polymerase gamma, enzyme; qPCR, quantitative PCR; RPKM, reads per kilobase of target per million reads; RT, room temperature; SD, standard deviation; SP, sodium pyruvate; TK2, thymidine kinase 2.

Laurence A. Bindoff and Kristina Xiao Liang share corresponding authorship.

This is an open access article under the terms of the [Creative Commons Attribution-NonCommercial-NoDerivs](https://creativecommons.org/licenses/by-nc-nd/4.0/) License, which permits use and distribution in any medium, provided the original work is properly cited, the use is non-commercial and no modifications or adaptations are made.

© 2023 The Authors. *The FASEB Journal* published by Wiley Periodicals LLC on behalf of Federation of American Societies for Experimental Biology.

Forskningsråd (Forskningsrådet),
Grant/Award Number: 229652 and
262613; Rakel og Otto Kr. Bruuns legat

significantly delayed in iNSCs carrying the compound heterozygous *POLG* mutations. In contrast, iNSC with the homozygous *POLG* mutation recovered their mtDNA at a rate similar to controls. When we treated cells with dNs, we found that this reduced EtBr-induced mtDNA depletion and significantly increased repopulation rates in both patient iNSCs. These observations are consistent with the hypothesis that mutations in *POLG* impair mtDNA repopulation also within intact neural lineage cells and suggest that those with compound heterozygous mutation have a more severe defect of mtDNA synthesis. Our findings further highlight the potential for dNs to improve mtDNA replication in the presence of *POLG* mutations, suggesting that this may offer a new therapeutic modality for mitochondrial diseases caused by disturbed mtDNA homeostasis.

KEYWORDS

deoxynucleosides, iPSCs, mitochondrial DNA replication, neural stem cells, polymerase γ , therapy

1 | INTRODUCTION

The nuclear-encoded enzyme DNA polymerase γ (Pol- γ) replicates and repairs mitochondrial DNA (mtDNA) and is therefore essential for mtDNA copy number homeostasis.¹ Mutations in *POLG*, the gene encoding the catalytic subunit of Pol- γ , cause a decline in catalytic activity and mtDNA copy number depletion.² *POLG* mutations are among the commonest causes of mitochondrial disease and are associated with a range of phenotypes.³ The autosomal recessive catalytic subunit mutations W748S and A467T are founder mutation in multiple populations, with a high prevalence in the Scandinavian and Finnish populations, and are commonly associated with disease in either a compound heterozygous or homozygous state.^{4,5}

The absence of robust models has impeded our understanding of disease pathogenesis and the development of treatments, which remain largely limited to symptomatic and supportive care.⁶ Our previous studies using human post-mortem brain tissue showed that *POLG*-related disease led to widespread damage in the brain with substantia nigra dopaminergic neurons being the most affected.^{7,8} However, post-mortem studies represent the terminal stages of disease and are not easily tractable. Further, animal models have often failed to recapitulate human neurological phenotypes.⁹ There is, thus, a clear need for robust models in the study of disease mechanisms and therapeutic development. Therefore, we chose to model *POLG*-related disease in induced pluripotent stem cells (iPSCs) that retain the potential to differentiate into any cell type and carry the patient's own genetic background.

The lack of effective treatments for mitochondrial disease has led to numerous studies focused on potential

new therapies, including molecules with antioxidant properties,^{10–12} metabolites designed to boost mitochondrial oxidative phosphorylation function^{13,14} or molecules that protect mitochondrial inner membrane phospholipids.^{15–17} As substrate availability in the form of deoxyribonucleotide triphosphates (dNTPs) is vital to sustain mtDNA replication, administration of dNTPs or their precursors, deoxyribonucleosides (dNs), has been shown to increase mtDNA copy number in a range of different cell types in vitro.^{18–21} Supplementation of dNs has also been used therapeutically to increase mtDNA copy number in patients with mitochondrial thymidine kinase 2 (TK2) deficiency, where they bypass the nucleotide generation defect in these patients.²² Further, in vitro studies conducted in *POLG* patient primary cells have suggested that increasing the dNTP pool could promote the improvement of mtDNA depletion.^{18,19}

In this current study, we used reprogrammed iPSC-derived neural stem cells (iNSCs) that were either homozygous for W748S (WS5A) or heterozygous for A467T/W748S (CP2A) and which we had previously shown recapitulated several molecular features found in post-mortem tissue studies, including loss of mtDNA copy number and MRC complex I.²³ We investigated how these cells responded to chemically induced depletion of their mtDNA by ethidium bromide (EtBr), a double-stranded DNA intercalating drug that effectively depletes mtDNA copy number in proliferating cells,²⁴ without affecting nuclear DNA at low concentration.^{25,26} Further, as this effect is reversible, cells are able to repopulate their mtDNA copy number after removal of EtBr.²⁷ Previous studies in fibroblasts showed that *POLG* patient cells failed to repopulate their mtDNA

copy number after EtBr-induced mtDNA depletion.²⁸ Since fibroblasts typically fail to manifest the mitochondrial dysfunction associated with POLG disease,²³ we applied a similar approach using POLG iNSCs to study what happens to mtDNA replication in neural lineage cells. We also asked whether increased dNTP availability driven by dN supplementation could modulate the depletion or repopulation of mtDNA in the same neural lineage cell type.

2 | MATERIALS AND METHODS

2.1 | Derivation of iPSCs

Patient and control fibroblasts were reprogrammed into iPSCs as previously described.²³ Fibroblasts were collected from two patients with different *POLG* mutations, homozygous c.2243G>C, p.W748S/W748S (WS5A) and compound heterozygous c.1399G>A/c.2243G>C, p.A467T/W748S (CP2A). Detroit 551 (ATCC® CCL 110™, human fetal female, control 1) and AG05836 (RRID:CVCL_2B58, 44 years old female, control 2), were used as the disease-free controls. All cells were collected with written informed consent from patients. Ethical approval for the project was granted by The Norwegian Research Ethics Committee (2012/919).

2.2 | Cell culture and neural induction

Cell culture and neural induction of iPSCs were conducted as described previously.²³ Tests for mycoplasma contamination were routinely conducted using a mycoplasma detection assay (Lonza, cat no. LT07-218). Multiple clones were used for both control and patient iNSC lines: two clones from Detroit 551 control, one clone from AG05836 control, three different WS5A patient iNSC clones, and two different clones from CP2A patient iNSCs.

2.3 | Flow cytometry

Cells were fixed with 1.6% PFA and permeabilized with ice-cold 90% methanol. Characterization of iNSCs was conducted using antibodies against neural progenitor markers PAX6 (Novus Biologicals, cat. no. NBP2-34705APC, 1:50) and Nestin (R&D Systems, cat. no. IC1259P, 1:200). All samples were analyzed on a BD Accuri™ C6 flow cytometer with 10 000 or more events were recorded per sample. Accuri™ C6 software was used for data analysis.

2.4 | Depletion of mtDNA by EtBr

All iNSCs lines were seeded into Geltrex-coated 24-well plates in NSC medium containing 0.1 mg/mL Sodium Pyruvate (SP) (Sigma, cat no. S8636) and 0.05 mg/mL uridine (Sigma, cat. no. U3003) at a density of approximately 100 000 cells per well and the day was recorded as day-1 (D-1). On day 0 (D0), DNA was extracted from one well of each plate using the QIAGEN DNeasy Blood and Tissue Kit (QIAGEN, cat. no. 69504) in accordance with the manufacturers protocol. The medium was then changed into an NSC medium containing 50 ng/mL EtBr and supplemented with 0.1 mg/mL SP and 0.05 mg/mL uridine. The cells were kept in a medium with EtBr for 7 days, with a medium change every 2 days. After 7 days, the EtBr medium was removed, the cells were washed with 2 mL DPBS without Calcium and Magnesium (DPBS–/–), and NSC medium supplemented with only SP and uridine was added. The cells were kept in this medium for 14 days (until D21), with changes of medium every 2 days. DNA was extracted from one well of each plate every day from D0 to D21 using QIAamp DNA Mini Kit (Qiagen, cat. no. 51304) and stored at –20°C. For each cell line/clone, untreated control plates were studied in parallel, and DNA was extracted every 4 days (D0, D4, D8, D12, D16, and D20).

2.5 | Treatment of iNSC with dNs

Cells were seeded in NSC medium containing 0.1 mg/mL SP and 0.05 mg/mL uridine on Geltrex-coated 24-well plates at a density of approximately 100.000 cells per well (D1). The cells were treated with NSC medium containing 50 ng/mL EtBr, 50 μM 2'-deoxyadenosine (Sigma-Aldrich, cat. no. D8668), 50 μM 2'-deoxythymidine (Sigma-Aldrich, cat. no. T1895), 50 μM 2'-deoxycytidine (Sigma-Aldrich, cat. no. D0776), 50 μM 2'-deoxyguanosine (Sigma-Aldrich, cat. no. D0901) and 5 μM EHNA (Sigma-Aldrich, cat. no. E114), supplemented with 0.1 mg/mL SP and 0.05 mg/mL uridine. Further, the iNSCs were kept in medium with EtBr for 7 days, with a change of medium every 2 days. After 7 days, the EtBr medium was removed and the cells were washed with DPBS–/– before the addition of NSC medium supplemented with only dNs, EHNA, SP, and uridine. The cells were cultured in this medium for 14 days (until D21), with changes of medium every 2 days. DNA was extracted from one well from each plate at D0, D3, D7, D11, D16, and D21 and stored at –20°C. For each cell line/clone, control plates only treated with dNs were studied in parallel, and DNA was extracted at the same time as for EtBr-treated plates.

2.6 | Immunocytochemistry

INSCs were cultured in six-well plates on Geltrex-coated coverslips and fixed by incubation with 4% (v/v) paraformaldehyde (PFA, VWR, cat. no. 100503 917). Cells were then immersed in blocking buffer containing 1× PBS, 10% (v/v) normal goat serum (Sigma-Aldrich, cat. no. G9023), and 0.3% (v/v) Triton™ X-100 (Sigma-Aldrich, cat. no. X100-100 ML), incubated with primary antibody solution overnight at 4°C and stained with secondary antibody solution (1:800 in blocking buffer) for 1 h at RT. INSCs were stained with rabbit Anti-PAX6 (Abcam, cat. no. ab5790, 1:100), mouse anti-Nestin (10c2) (Santa Cruz Biotechnology, cat. no. sc23927, 1:50) and rabbit anti-SOX2 (Abcam, cat. no. ab97959, 1:100). The secondary antibodies used were Alexa Flour® goat anti-rabbit 488 (Thermo Fisher Scientific, cat. no. A11008, 1:800) and Alexa Flour® goat anti-mouse 594 (Thermo Fisher Scientific, cat. no. A11005, 1:800). After secondary antibody incubation, the coverslips were mounted onto cover slides using Prolong Diamond Antifade Mountant with DAPI (Invitrogen, cat. no. P36962).

2.7 | MtDNA copy number quantification by qPCR

Total DNA was extracted using a QIAGEN DNeasy Blood and Tissue Kit (QIAGEN, cat. no. 69504) according to the manufacturer's protocol, and the concentration of each sample was quantified by spectrophotometry (NanoVue Plus™, Biochrom). Quantification by qPCR was conducted by amplification of the mitochondrial gene ND1 and nuclear single copy gene APP. The sequencing of the primers and probes were: ND1 forward primer 5'-CCCTAAAACCCGCCACATCT-3' (location L3485-3504), ND1 reverse primer 5'-GAGCGATGGTGAGAGCTAAGGT-3' (location H3553-3532), ND1 probe 5'-6FAM-CCATCACCTCTACATCACCGCCC-3' (TaqMan-MGB, Location L3506-3529), APP forward primer 5'-TGTGTGCTCTCCAGGTCTA-3', APP reverse primer 5'-CAGTTCTGGTCACTGG-3', APP probe 5'-VIC-CCCTGAACTGCAGATCACCAATGTGGTAG-3' (TaqMan-MGB). A master mix containing 1X of 2X TaqMan™ Fast Advanced Master Mix (ABI, cat. no.: 4444964), 10 μM ND1 forward primer, 10 μM ND1 reverse primer, 5 μM ND1 probe (TaqMan-MGB), 10 μM APP forward primer, 10 μM APP reverse primer and 5 μM APP probe (TaqMan-MGB) was prepared in MilliQ. A 10 ng/μL DNA template was added to each well of a 96-well plate containing the master mix. MilliQ was used as a negative control and DNA from the commercial fibroblast line Detroit 551 (ATCC® CCL 110™)

was used as internal control. Plates were centrifuged at 400 g for 1 min before RT-qPCR was run using the Applied Biosystems™ 7500 Fast Real Time PCR system with the following program: 20-s initial denaturation at 95°C, 3-s denaturation at 95°C and 30-s primer and probe hybridization and DNA synthesis at 60°C. The last two steps were repeated for 40 cycles. Analysis of Ct-values was done in Microsoft Excel and used to calculate estimated expressions.

2.8 | RNA sequencing

RNA was extracted at D0, D7, and D21 using the RNeasy extraction kit (QIAGEN, cat no. 74104) according to the manufacturer's protocol, and the concentration of each sample was measured by spectrophotometry (NanoVue Plus™, Biochrom).

Library preparation (BGISEQ-500RS High-throughput sequencing kit, PE50, V3.0, MGI Tech Co, Ltd, Shenzhen, China), hybridization, and sequencing were performed at BGI (Shenzhen, China) in accordance with their standard procedure. Sequencing was done at BGI using BGISEQ-500 and the sequencing data was filtered using the SOAPnuke (v1.5.2) software. Mapping of the processed FASTQ files to the human trainSCriptome and genome was performed using HISAT2 (v2.0.4). The genome version was GRCh38, with annotations from Bowtie2 (v2.2.5). Gene expression levels were calculated by RSEM (v1.2.12) software.

For RNA sequencing analysis, the set of differentially expressed genes (DEGs) identified from pairwise comparisons was identified using Deseq2 (v1.4.5) package (BGI, Wuhan, China). The number of reads per kilobase per million reads (RPKM) method was used to calculate the modification levels of unique genes. Significantly DEGs were defined as ones with at least 0.3 FPKM level of expression in at least one of the conditions and a *q*-value less than .05 by the Bonferroni test. KEGG (<https://www.kegg.jp/>) enrichment analysis of annotated DEGs was performed by Phyper (https://en.wikipedia.org/wiki/Hypergeometric_distribution) based on Hypergeometric test.

2.9 | Statistical analysis

Statistical analyses were carried out utilizing IBM SPSS Statistics 27 (SPSS Inc., Chicago, USA). Data distribution was evaluated via the Shapiro–Wilk test, which indicated that the data were not normally distributed. As a result, comparisons were made using the Mann–Whitney *U* test. Differences were deemed statistically significant at the following levels: **p* < .05; ***p* < .01; ****p* < .001; *****p* < .0001. GraphPad Prism 8 (GraphPad Software, USA) was

employed for data visualization, and results are displayed as mean \pm standard deviation (SD) for sample sizes of three or more ($n \geq 3$).

3 | RESULTS

3.1 | EtBr treatment causes significant depletion of mtDNA in control and patient iNSCs

We differentiated iPSCs reprogrammed from human skin fibroblasts into iNSCs as previously described.²³ Five days after neural induction, iPSCs reached a neural epithelial stage and were subsequently lifted into neural spheres in suspension culture. Further, the spheres were dropped into monolayer iNSCs (Figure 1A). Validation of neural lineage by immunostaining showed that iNSCs expressed specific neural progenitor markers PAX6 and Nestin (Figure 1B,C) with >97% of the cells displaying positive staining for both (Figure 1C).

To investigate the effect of forced mtDNA depletion, we treated control and patient iNSCs with EtBr (Figure 1D) for 7 days with untreated iNSC of each run in parallel. Following EtBr removal, cells were cultured for an additional 14 days (D21) in the absence of EtBr (Figure 1E). DNA was extracted from EtBr-treated cells every day (D0–D21) and every 3–4 days from untreated iNSCs. During the 7 days of EtBr treatment, a decrease in growth rate and cell viability was observed for all cell lines, however, no change in morphology was detected for either controls or patient iNSCs from D0 to D21 (Figure S1).

Both control lines showed a marked depletion of mtDNA, occurring as early as after 24 h (D1) (Figure 2A, Table S2). After 7 days of treatment, mtDNA levels had dropped to between 80% and 90% of starting levels, while mtDNA in untreated controls remained steady (Figure 2A,B, Table S2). EtBr-treated POLG iNSCs showed 78% (WS5A) and 85% (CP2A) mtDNA depletion after 7 days (Figure 2C,D, Table S2), while untreated patient iNSCs cultured in parallel showed no significant change (Figure 2D, Table S2). Following the removal of EtBr, both control lines were able to repopulate their mtDNA back to pre-treatment levels (Figure 2E, Table S3). Interestingly, the rate of repopulation for mutated WS5A iNSCs was similar to controls, and mtDNA levels in both increased to levels that exceeded initial (D0) amounts following release from depletion. This initial overshoot was followed by correction to pre-treatment levels (Figure 2F,G, Table S2 and S3). The compound heterozygous CP2A iNSCs did not, however, recover their mtDNA content: the amount of mtDNA stabilized at approximately 78% compared to D0 (Figure 2F,G, Table S2 and S3) and showed no initial overshoot.

3.2 | POLG patient iNSCs show increased numbers of differentially expressed genes after EtBr treatment

To explore the reasons behind the differential response in patient lines, we investigated changes in gene expression during and after EtBr treatment. We performed RNA sequencing from samples extracted at three different time points: before treatment (D0), after 7 days of EtBr treatment (D7), and 14 days after stopping treatment (D21). Additionally, RNA sequencing of untreated parallels was performed.

When comparing EtBr-treated and -untreated iNSCs, numerous significant DEGs were found at D7 in all lines (Figure 3A,B). However, while both patient lines (Figure 3B) showed increased numbers of DEGs compared to controls (Figures 3A and S3A–D), the number of upregulated (3644) and downregulated genes (3076) was much higher in WS5A than in both CP2A (up: 2630, down: 2465) and controls (Control 1—up: 140, down: 344; Control 2—up: 301, down: 246).

After 14 days without EtBr, D21, very few DEGs remained in either control line compared to untreated parallels (Figure 3A): in control 1, only 3 genes were found to be upregulated and 4 genes downregulated compared to untreated iNSCs, and in control 2, 17 genes were upregulated, and 5 genes downregulated. In contrast, a much larger number of DEGs remained in both WS5A and CP2A iNSCs compared to their untreated parallels (Figures 3B and S3E–H): in WS5A, 541 upregulated genes and 687 downregulated genes, and in CP2A 165 genes were upregulated and 86 genes downregulated. This indicates that EtBr treatment of both controls had almost completely recovered after 14 days while the POLG patient iNSCs still showed clear signs of dysregulated gene expression.

3.3 | Dysregulation of metabolic pathways in POLG patient iNSCs

In order to investigate the potential mechanisms underlying the gene expression differences seen in patient cell lines following recovery from EtBr treatment, we used KEGG pathway classification analysis. Combining the DEGs between EtBr-treated and -untreated iNSCs from post-treatment time points (D7 and D21, Figure S2), we found that dysregulated genes were distributed mainly in autophagy/mitophagy (control 1: 72/73; control 2: 109/108; WS5A: 1420/1467; CP2A: 1066/1088) and metabolic pathways (control 1: 32; control 2: 55; WS5A: 610; CP2A: 432) (Figure 3C,a–d). Further KEGG pathway enrichment of metabolic pathways DEGs showed that genes related to purine and pyrimidine nucleotide metabolism appeared

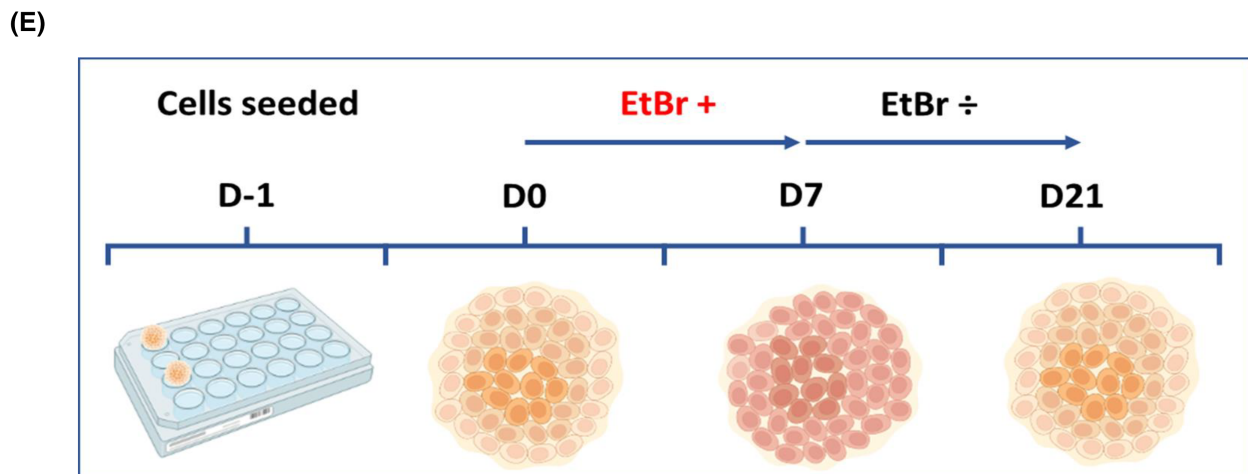
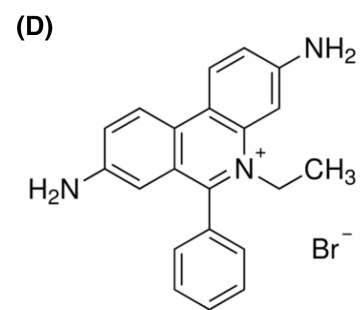
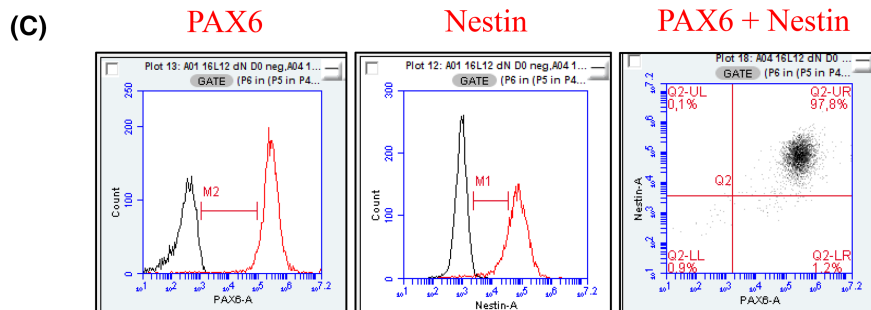
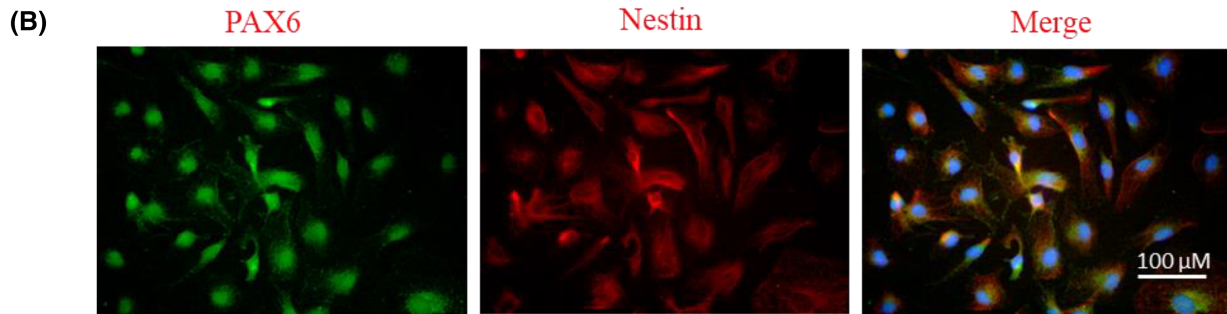
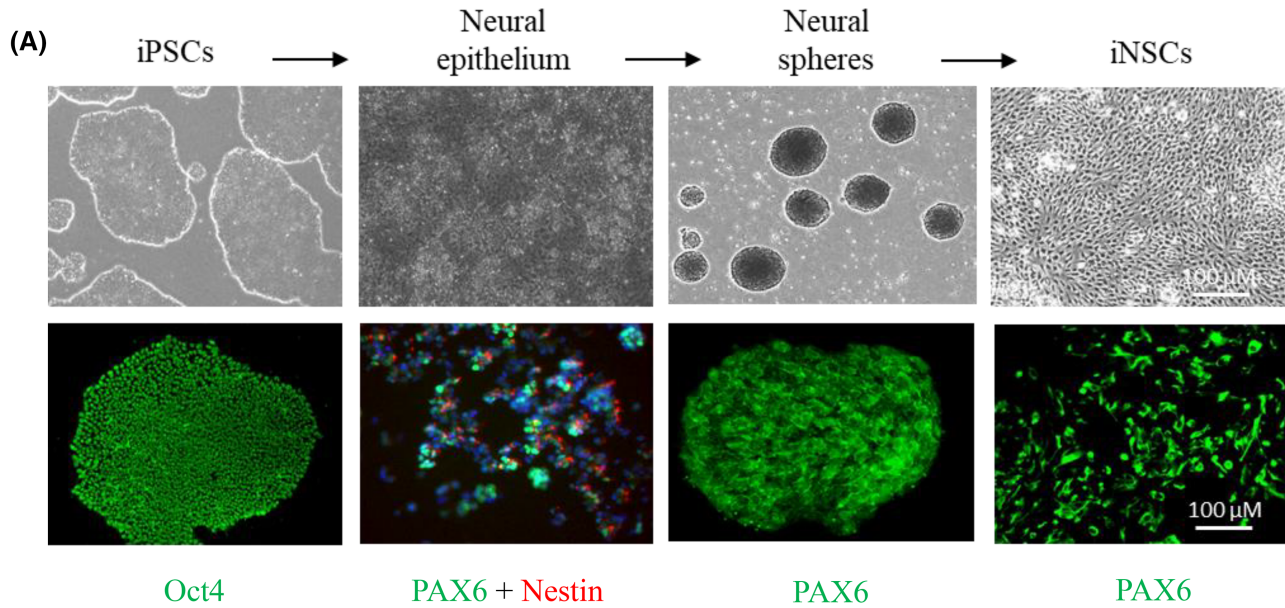


FIGURE 1 Generation of iNSCs and overview of EtBr treatment setup. (A) Upper panel: Morphology of cells at different stages of iNSC differentiation, from the neural induction of iPSCs through an intermediate neural epithelial stage and into suspension culture neural spheres before dissociation into monolayer iNSCs. Lower panel: Immunostaining for specific stages during neural induction, including Oct4 positive iPSCs (green), Nestin (red) and PAX6 (green) expressing neural epithelium, and neural spheres and monolayer iNSCs expressing PAX6 (green). Scale bar: 100 μ m. (B) Immunofluorescent staining of iNSCs displaying positive expression of neural progenitor markers PAX6 and Nestin. Nuclei were counterstained with DAPI. Scale bar: 100 μ m. (C) Flow cytometric analysis of iNSCs showing >97% positive marker expression for both single and co-staining of PAX6 and Nestin. (D) EtBr molecular structure. (E) Graphical overview of EtBr treatment in NSCs from cell seeding (D-1), introduction of EtBr to the growth medium (D0), stop of treatment (D7) and recovery period (D7–D21). Created with BioRender.com.

differentially expressed in all cell lines (Figure 3D,a–d): after 1 week of EtBr treatment (D7), alterations in nucleotide metabolism-related genes were present in both controls and patient lines. Two weeks after treatment, however, only one gene remained differentially expressed in control 1 and none in control 2, while multiple DEGs were still present in both patient lines, particularly in WS5A (Table S1).

Selecting the DEGs under the purine and pyrimidine nucleotide metabolism pathways, we then compared the gene expression profiles of the patients. All four DEGs, deoxythymidylate kinase (*DTYMK*), ribonucleoside diphosphate reductase (*RRM1*) (Figures 3E,a,b and S4), DNA polymerase delta 1 (*POLD1*), and DNA polymerase epsilon subunit 3 (*POLE3*) (Figure S4, Table S1) were significantly downregulated in EtBr-treated CP2A iNSCs at D21 compared to untreated iNSCs. In contrast, both upregulated and downregulated genes were found in EtBr-treated WS5A iNSCs at D21, including ribonucleotide reductase regulatory TP53 inducible subunit M2B (*RRM2B*), Inosine Monophosphate Dehydrogenase 2 (*IMPDH2*), Cytidine/Uridine Monophosphate Kinase 1 (*CMPK1*), Adenylate kinase 2 (*AK2*) and 4 (*AK4*) and NME/NM23 Nucleoside Diphosphate Kinase 4 (*NME4*) (Figure S4). However, several of these genes showed significantly higher expression in WS5A compared to both controls and CP2A and, interestingly, this increased expression was present prior to EtBr treatment (Figure S4). When we investigated expression levels of multiple genes important for nucleotide metabolism (Figure 4B), we found that many were either upregulated in WS5A or downregulated in CP2A at D0 compared to controls (Figure 4A, Table S4).

3.4 | dN supplementation significantly increases mtDNA copy number in iNSCs with *POLG* mutations after EtBr-induced mtDNA copy number depletion

Given the specific dysregulation of genes involved in nucleotide metabolism, we asked whether supplementation with dNTP precursors, dNs, would counter the effects of

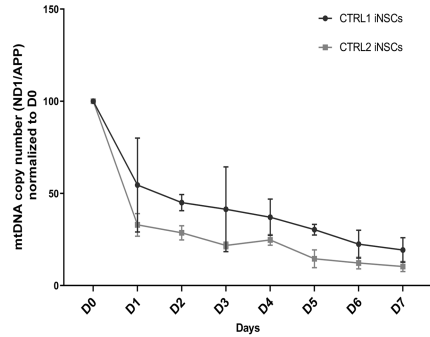
EtBr and potentially increase mtDNA copy number, particularly in CP2A. In order to assess if dNs both increased mtDNA copy number protected and against depletion, we co-treated iNSCs with EtBr and deoxyadenosine (dA), deoxythymidine (dT), deoxyguanosine (dG) and deoxycytidine (dC) (Figure 4C) and continued dN treatment for 14 days after EtBr treatment was stopped (D21).

The addition of dNs during EtBr treatment not only significantly increased the rate of mtDNA repopulation following EtBr removal, doing so in all cell lines, but particularly *POLG* patient iNSCs, it also protected against depletion (Figure 4D,E, Table S5). In CP2A iNSCs, which previously failed to repopulate completely their mtDNA copy number after EtBr removal, there was a 4-fold increase of mtDNA after dN treatment compared to D0 (Figure 4D, Table S5). A similar increase was seen in WS5A (5-fold compared to D0), while control iNSCs also displayed a 2-fold increase following EtBr removal in the presence of dNs (Figure 4D, Table S5). The addition of dNs together with EtBr treatment significantly reduced mtDNA depletion in WS5A from 79% to 30% (D7), and appeared to counteract the effect of EtBr in controls for the first 4 days of treatment, with minor depletion being seen only after D4 (Figure 4D,E, Table S5). In CP2A, depletion was reduced from 83% to 73% (D7), however, this did not reach significance (Figure 4E, Table S5).

Given our earlier observation that *POLG* iNSCs reiterate the mtDNA depletion found in post-mortem neurons from patients,²³ we wanted to investigate whether dN supplementation could also increase mtDNA copy number in EtBr untreated *POLG* iNSCs. Following 21 days dNs treatment, all iNSC lines showed increased mtDNA copy number, which appeared as early as D4 after start of treatment (Figure 4F, Table S6). However, while mtDNA levels in controls and CP2A patient iNSCs seemed to stabilize from D12, WS5A mtDNA continued to increase throughout treatment (Figure 4F, Table S6). Lastly, we compared all treatment conditions including EtBr-iNSCs, EtBr-dN-iNSCs, and dN-iNSCs (Figure 4G–I, Table S6). In all dN-treated cell lines, mtDNA content seemed to stabilize at a similar time point, regardless of EtBr treatment, but at a level higher than iNSCs treated only with EtBr.

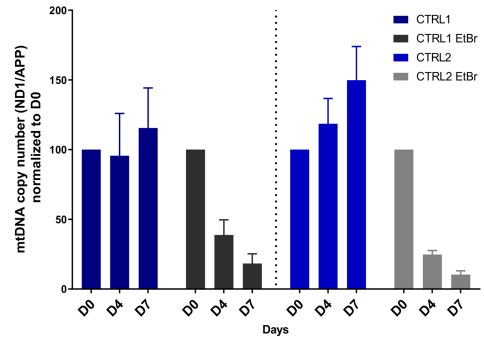
(A)

mtDNA copy no depletion in CTRL iNSCs during EtBr treatment



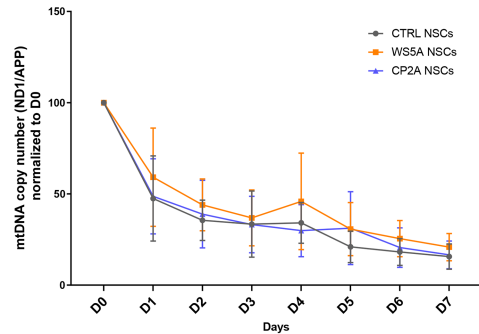
(B)

mtDNA copy no. in EtBr treated and untreated CTRL iNSCs



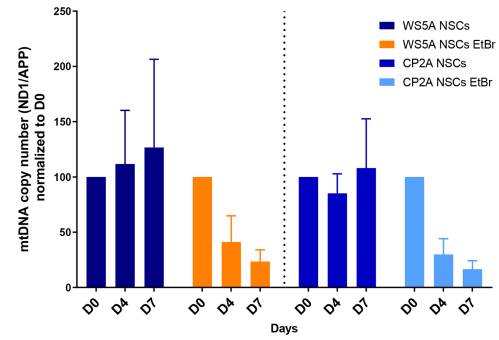
(C)

mtDNA copy no. depletion in EtBr treated WS5A and CP2A patient iNSCs vs CTRL



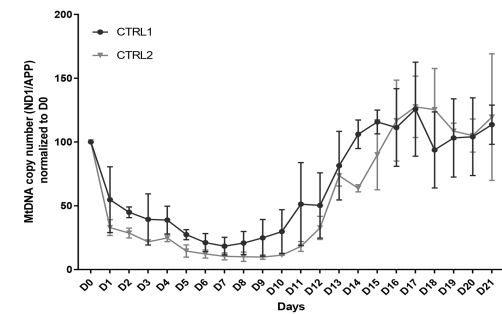
(D)

mtDNA copy no. in EtBr treated and untreated WS5A and CP2A patient iNSCs



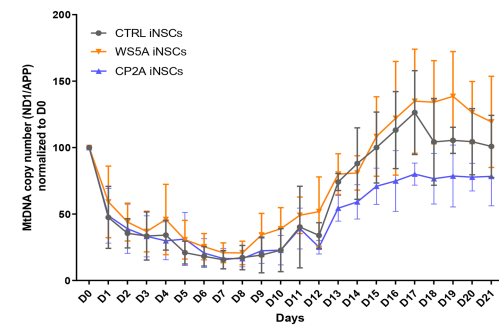
(E)

mtDNA copy no. change in EtBr treated WS5A and CP2A CTRL iNSC lines



(F)

mtDNA copy no. change in EtBr treated WS5A and CP2A patient iNSCs vs CTRL



(G)

mtDNA copy no. change in EtBr treated and untreated POLG iNSC lines vs CTRL

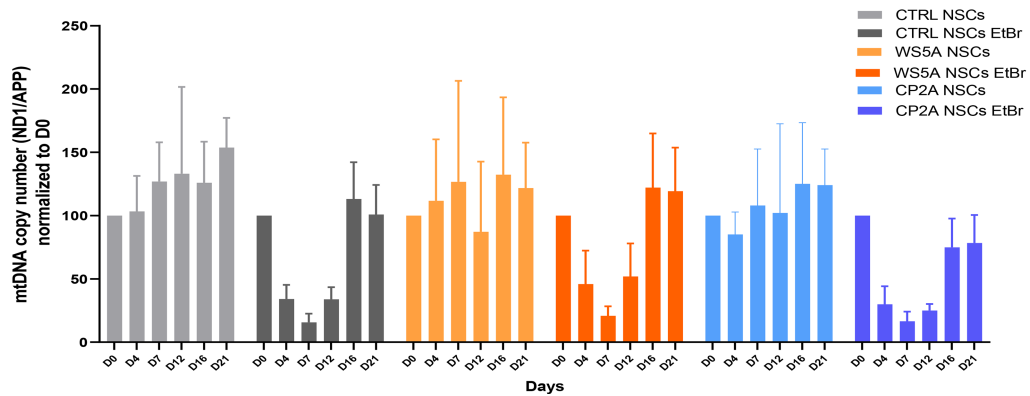


FIGURE 2 EtBr-induced mtDNA depletion and post-treatment recovery in *POLG* iNSCs. (A, B) MtDNA copy number depletion in control iNSCs during EtBr treatment over a 7-day period (A) and comparison of EtBr-treated and -untreated control iNSCs during the same period (B). (C, D) MtDNA copy number depletion in WS5A and CP2A patient iNSCs compared to control during EtBr treatment (C) and comparison of EtBr-treated and -untreated patient iNSCs during the same period (D). (E, F) EtBr-induced mtDNA copy number depletion (D0–D7) and subsequent repopulation (D7–D21) in control iNSCs (E) and in patient iNSCs compared to control (F). (G) MtDNA copy number in EtBr-treated control and patient iNSCs during treatment and recovery stages compared to their corresponding untreated iNSCs. Data are presented as mean \pm SD for the number of samples $n \geq 3$. All *p*-values are summarized in [Table S2](#).

4 | DISCUSSION

In this study, we used the paradigm of forced mtDNA depletion with EtBr to study mtDNA homeostasis in stem cells of neural lineage carrying founder *POLG* mutations, one homozygous for W748S and one compound heterozygous with W748S/A467T. We found that while mtDNA depletion occurred at similar rates, in both patient and control iNSCs, mtDNA repopulation showed a significant difference between cells with different *POLG* genotypes: compound heterozygous iNSCs showed a distinct delay in repopulation and a failure to recover mtDNA to pre-treatment levels. RNA-seq studies identified preexisting differences in the expression of genes involved in nucleotide metabolism that potentially explained the greater ability of homozygous cells to withstand EtBr-induced depletion. Supplementation with dNs improved not only mtDNA repopulation, by promoting higher levels than pre-treatment, it also protected cells against depletion during EtBr exposure.

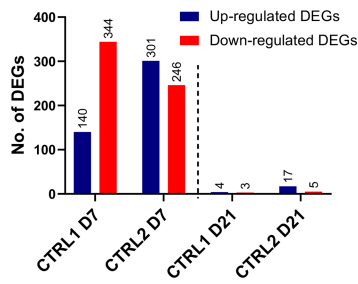
POLG-related diseases are among the most common genetically determined mitochondrial disorders and while the manifestations vary, involvement of the central nervous system, particularly with devastating epilepsy,³ is very common. We chose, therefore, to investigate mtDNA response to chemically enforced depletion in cells of neural origin that we have shown express the same molecular changes present in neurons taken post-mortem.²³ Further, since our clinical studies identified clear differences in survival based on *POLG* genotype, with compound heterozygotes having a worse prognosis than those with homozygous *POLG* mutations,³ we wanted to compare the response in neural stem cells containing relevant genotypes. The W748S and A467T are founder mutations that occur in multiple populations, and we used cells that were homozygous for the commonest, W748S (WS5A), and compound heterozygous for W748S/A467T (CP2A), a frequently found combination.

EtBr is a well-known DNA intercalating agent often used in molecular biology, particularly in visualizing DNA in agarose gel electrophoresis. While it can bind to all types of DNA, including both mtDNA and nuclear DNA (nDNA), it has been used experimentally to preferentially affect mtDNA when applied at low concentrations. This selective

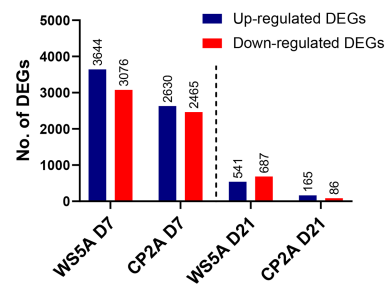
impact arises not because of EtBr's inability to permeate the nuclear membrane of intact cells, but due to a combination of several factors. Firstly, the double-membrane structure of the mitochondria allows EtBr to accumulate in higher concentrations within the mitochondrial matrix compared to the cell cytoplasm due to the highly negative mitochondrial membrane potential. This causes the relative concentration of EtBr to be higher in the mitochondria than in the nucleus. Secondly, mitochondria lack the advanced DNA repair mechanisms found in the nucleus. Hence, any damage to the mtDNA caused by EtBr intercalation is less likely to be effectively repaired, leading to a preferential loss or depletion of mtDNA over time under low-concentration EtBr treatment. Finally, the nuclear envelope does offer some degree of protection to nDNA. The nuclear envelope is a double membrane structure that separates the nucleus from the cytoplasm and regulates the passage of molecules in and out of the nucleus. While EtBr can enter the nucleus, the nuclear envelope may reduce the rate at which it does so, contributing to the relative preservation of nDNA under low-concentration EtBr treatment. However, it is important to note that at higher concentrations, EtBr can and does cause significant damage to nuclear DNA.^{29–31} Therefore, care must be taken to ensure that experimental conditions using EtBr to selectively affect mtDNA are carefully controlled.

In our study, the EtBr efficiently depleted cells of mtDNA at a low concentration of 50 ng/mL and the rate and extent were similar in all cells irrespective of genotype. Repopulation of mtDNA began around Day 12, both in patients and controls, and there was a consistent overshoot in the control lines that was also present in WS5A cells ([Figure 2F](#)). Indeed, controls and WS5A achieved pretreatment levels of mtDNA usually by day 15 and levels in excess of this for the remainder of the study period (5–6 days). This did not happen in CP2A cells. MtDNA did begin to increase on Day 12, but repopulation failed to reach pre-treatment levels even by Day 21. Based on previous studies, we knew that both WS5A and CP2A cells had a lower than normal starting level of mtDNA and complex I and that this was most severe in CP2A.²³ These initial experiments confirmed, therefore, that there are indeed molecular phenotypic differences induced by *POLG* genotype, but they provided no causal mechanistic explanation.

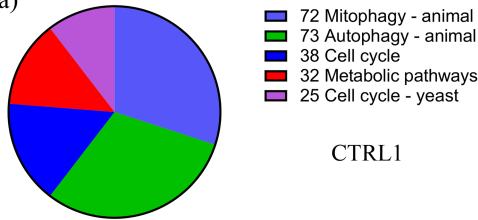
(A) DEGs in untreated vs EtBr treated CTRL INSCs



(B) DEGs in untreated vs EtBr treated POLG INSCs



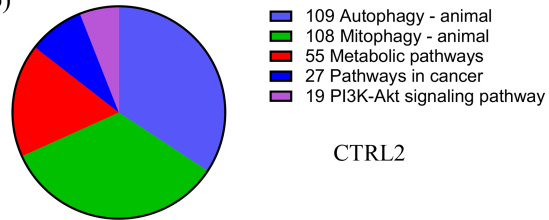
(C) a)



CTRL1

Total=240

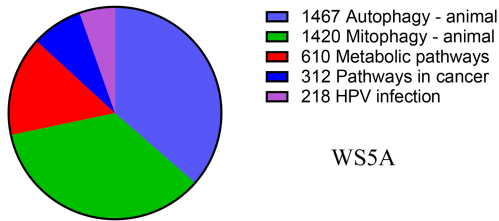
b)



CTRL2

Total=318

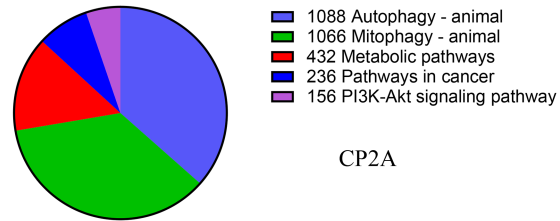
c)



WS5A

Total=4027

d)

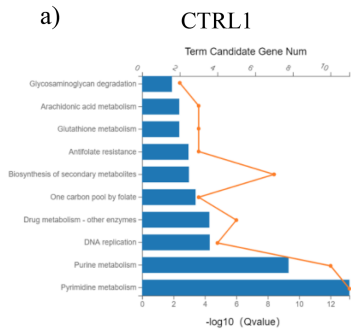


CP2A

Total=2978

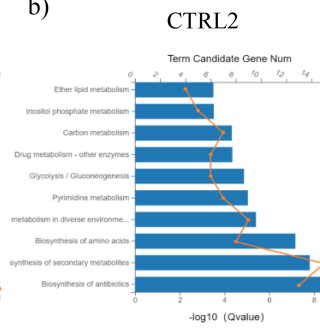
(D)

a)



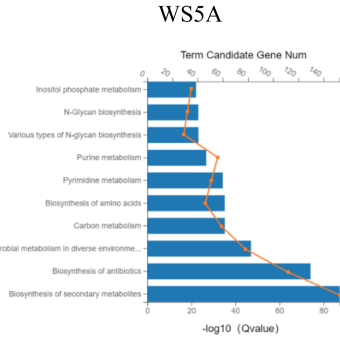
CTRL1

b)



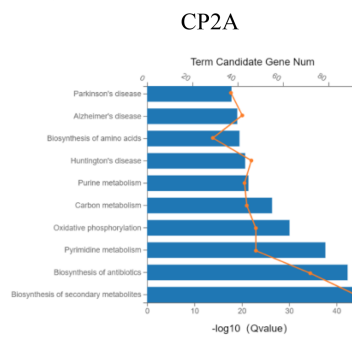
CTRL2

c)



WS5A

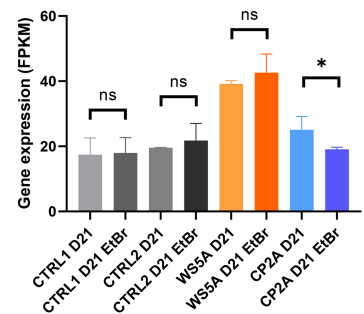
d)



CP2A

(E)

a) *DTYMK* expression at D21 in EtBr treated and untreated CTRL and POLG NSCs



b)

RRM1 expression at D21 in EtBr treated and untreated CTRL and POLG NSCs

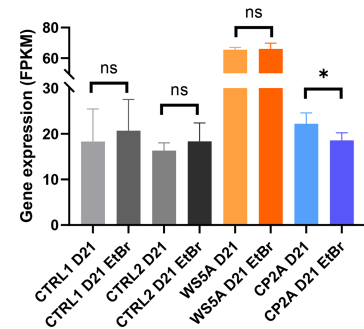


FIGURE 3 Alterations in POLG iNSC gene expression during and after EtBr treatment. (A, B) Number of up- and downregulated genes in EtBr-treated vs -untreated iNSCs after 7 days EtBr treatment (D7) and after two weeks of recovery (D21) for control iNSCs (A) and patient iNSCs (B). (C) Top 5 differentially expressed pathways in EtBr-treated CTRL1 (a), CTRL2 (b), WS5A (c) and CP2A (d) iNSCs from KEGG Pathway Classification analysis. (D) KEGG Pathway Enrichment analysis showing the top 10 differentially expressed metabolic pathways between EtBr-treated and -untreated CTRL1 (a), CTRL2 (b), WS5A (c) and CP2A (d) iNSCs. (E) Gene expression of top nucleotide metabolism-related DEGs between EtBr-treated and -untreated CP2A iNSCs at D21, including (a) *DTYMK* (Deoxythymidylate kinase) and (b) *RRM1* (Ribonucleotide reductase, alpha subunit). Data are presented as mean \pm SD for the number of samples $n \geq 3$. * $p < .05$.

To explore the differential response seen in patient lines, we used RNA-seq to investigate changes in gene expression during and after EtBr treatment. While some findings were expected, e.g., dysregulation of autophagy/mitophagy, analysis of EtBr-treated iNSCs showed a clear differential response between POLG patients and controls, and especially between patient lines, of genes involved in purine and pyrimidine nucleotide metabolism, several of which were already known causes of mtDNA depletion syndromes such as *DTYMK*³² and *RRM2B*.³³ We found that all DEGs, including *DTYMK*, was significantly downregulated in CP2A EtBr-treated iNSCs at D21 while in WS5A, both up- and downregulated genes related to nucleotide synthesis were found. Further, several of these genes had significantly higher expression in both EtBr-treated and -untreated WS5A iNSCs when compared to controls and CP2A: put another way, the increased expression of these genes was already present in WS5A iNSCs prior to treatment with EtBr. When we investigated expression levels of other genes important for nucleotide metabolism at D0, we found that many of these were either upregulated in WS5A or downregulated in CP2A compared to controls (Figure 4A). These findings suggest that the relative balance of expressed genes in the pathways serving nucleotide synthesis can predict the differential response to mtDNA stress. On a clinical level, this implies that patient-specific regulation of nucleotide metabolism-related genes can impact that individual's mtDNA replication rate and thereby the response to mtDNA depletion. This could, in part, also explain why some patients are more severely affected than others.

While mitochondria have their own pathway for dNTP salvage, they also rely on import of dNTPs from de novo synthesis in the cytosol. Therefore, dNTP availability is vital for maintaining mtDNA replication rate and fidelity, especially in quiescent and post-mitotic cells where dNTP pools are reduced by diminished cytosolic synthesis.³⁴ Increasing the concentration of dNTPs through supplementation improves mtDNA replication also in cells with POLG mutations that decrease dNTP affinity.¹⁸ Previous studies also show that the Y955C *POLG* mutation has strongly impaired DNA synthesis activity that can be partly overcome at high dNTP concentrations.³⁵ In our study, we found that treatment with dNs significantly improved mtDNA copy number repopulation in EtBr-treated

POLG WS5A and CP2A iNSCs. This is particularly interesting in the case of the compound heterozygous CP2A line, which was unable to recover to pre-treatment mtDNA levels after EtBr treatment. Even in this cell line, however, supplementation with dNs during and after EtBr treatment gave a 4-fold increase in mtDNA compared to D0. Supplementation with dNs not only restored mtDNA content in CP2A following mtDNA depletion, but it also increased mtDNA to above pre-treatment levels in all iNSCs lines, including control lines. This supports the concept of dNTP concentration being rate limiting for mtDNA replication in cells affected by mitochondrial depletion disorders,^{18,36,37} and one that might be overcome by supplementation of dNs to boost dNTP availability.

Our results show that it is possible to normalize mtDNA levels irrespective of POLG genotype, including in very affected cell lines (CP2A), and highlights how providing POLG with sufficient substrate (dNTP) influences how cells respond to the presence of a dysfunctional polymerase gamma. The gene expression differences we observed also suggest that nucleotide metabolism, like many other biological variables, has a reserve capacity that is potentially manipulable. Indeed, the response seen in controls lines suggests that it should be possible to increase mtDNA levels by dNTP supplementation in many if not most instances. While we did not address the question of whether substrate excess leads to an increased error rate, this was investigated in an earlier study¹⁸ and their results suggest this is not the case. We believe, therefore, that dNTP supplementation is a potential therapy for POLG-related disease that should be investigated as soon as possible.

This study, in combination with the previously published findings,³⁸ has significantly advanced our understanding of the pathological mechanisms behind POLG mutations and the effect they have on mtDNA maintenance, particularly in NSCs. The current research identified a notable difference in the ability to restore mtDNA levels in iPSC-derived NSCs carrying compound heterozygous *POLG* mutations, in comparison to both controls and homozygous mutation carriers. This discovery aligns well with the previous study,³⁸ which also highlighted a greater mitochondrial functional impairment in compound heterozygous NSCs compared to their homozygous counterparts. While both studies agree on the

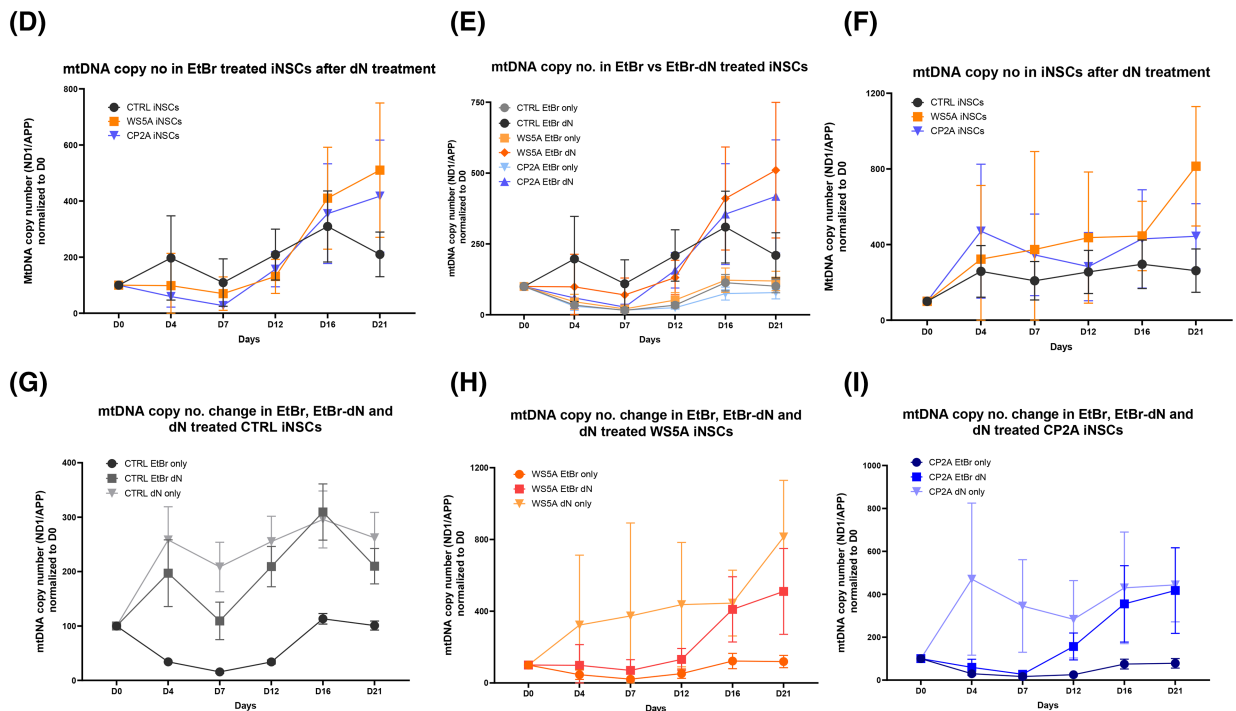
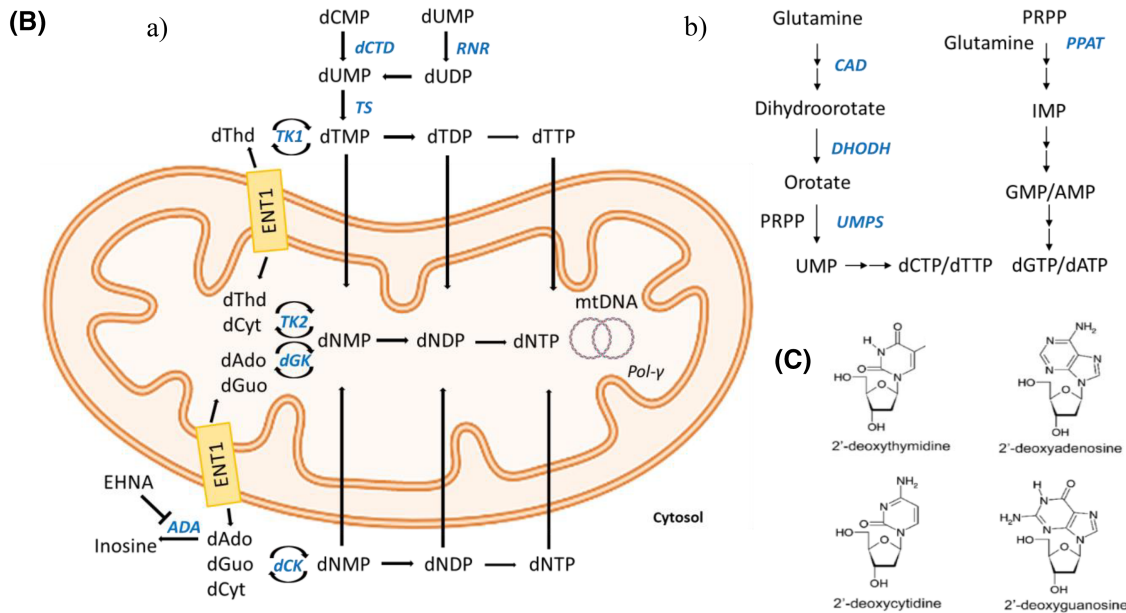
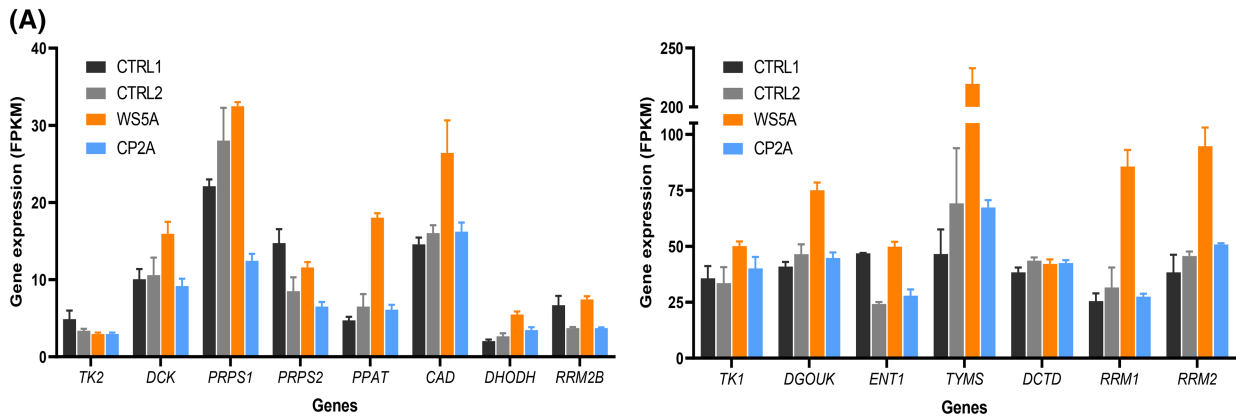


FIGURE 4 Supplementation with dNs improves mtDNA copy number repopulation in EtBr-treated POLG iNSCs. (A) Comparison of the gene expression of major nucleotide metabolism-related genes in all untreated (D0) iNSC lines. *DCTD*: Deoxycytidylate deaminase, *ENT1*: Equilibrative nucleoside transporter 1, *DGUOK*: Deoxyguanosine kinase, *TK2*: Thymidine kinase 2. *p*-Values are shown in Table S4. (B) Schematic overview of the main pathways for import and salvage of dNTPs in mitochondria (a) and cytosolic de novo dNTP synthesis (b). Major enzymes are depicted in blue. Abbreviations with bracketed encoding genes: ADA: Adenosine deaminase (*ADA*), dAdo: Deoxyadenosine, CAD: Carbamoyl-phosphate synthetase 2 (*CAD*), dCTD: Deoxycytidylate deaminase (*DCTD*), dCyt: Deoxycytidine, dCK: Deoxycytidine kinase (*DCK*), DHODH: Dihydroorotate dehydrogenase (*DHODH*), EHNA: erythro-9-(2-hydroxy-3-nonyl) adenine, ENT1: Equilibrative nucleoside transporter 1 (*ENT1*), dGuo: Deoxyguanosine, dGK: Deoxyguanosine kinase (*DGUOK*), NDPK: Nucleotide diphosphate kinase, PPAT: Phosphoribosyl pyrophosphate (PRPP) amidotransferase (*PPAT*), RNR: Ribonucleotide reductase (*RRM1*; alpha subunit, *RRM2/2B*: beta subunit isoforms) dThd: Thymidine, TK1: Thymidine kinase 1 (*TK1*), TK2: Thymidine kinase 2 (*TK2*), TS: Thymidylate synthase (*TYMS*), UMPS: Uridine monophosphate synthase (*UMPS*). Figure created with BioRender.com. (C) Molecular structures of deoxyribonucleosides thymidine, adenosine, guanosine and cytidine. (D) MtDNA copy number changes in control (CTRL), WS5A and CP2A iNSCs during co-treatment of EtBr and dNs (D0-D7) and dNs only (D7-D21). (E) Comparison of mtDNA content in EtBr-treated iNSCs and iNSCs co-treated with EtBr and dNs. (F) MtDNA copy number increase in iNSCs treated only with dNs over a period of 3 weeks. (G–I) Comparison of mtDNA copy number in iNSCs treated with EtBr, dNs, and co-treated with EtBr and dNs, in CTRL (G), WS5A (H) and CP2A (I) patient iNSCs. Data are presented as mean \pm SD for the number of samples $n \geq 3$. All *p*-values for Figure 4D–I are summarized in Tables S5 and S6.

more severe impact of compound heterozygous *POLG* mutations in NSCs, it's intriguing to note the differences in manifestations across different cell types. The previously published findings,³⁸ reported no observed functional differences between compound heterozygous and homozygous mutations in fibroblasts, iPSCs, or astrocytes, emphasizing the vulnerability of NSCs in the context of *POLG* mutations. In this study, the use of EtBr to induce mtDNA depletion, followed by studying repopulation rates in the current study, offers a functional perspective to support the earlier observations³⁸ regarding the disturbance of mtDNA copy number. Moreover, the current findings suggest a potential therapeutic approach, as dNs supplementation was found to mitigate the effects of EtBr-induced mtDNA depletion and improve repopulation rates in both patient-derived NSCs. This therapeutic strategy might have broad implications, given the pervasive role of *POLG* in mitochondrial diseases. In conclusion, the observations from the present study and our previous paper³⁸ underline the complexity of the cellular response to *POLG* mutations, dependent not only on the type of mutation (homozygous or compound heterozygous) but also the specific cell lineage. These discoveries pave the way for more targeted therapeutic strategies. They also emphasize the importance of studying these mutations in a range of cell types, especially those most affected in *POLG*-related diseases, to provide a more comprehensive understanding of disease pathophysiology and develop more effective treatment approaches.

Animal models have been invaluable tools for enhancing our comprehension of diseases, including *POLG*-related disorders, and evaluating potential treatments.³⁹ Despite this, they often fall short in accurately replicating human disease phenotypes due to inherent species-specific differences in physiology, genetics, and

immune responses. Although animal models, particularly rodent models, have been utilized to study *POLG* diseases, the manifestations of these diseases in animals often differ from their human counterparts, which can limit the translational potential of these studies. Nonetheless, preclinical animal models offer distinct advantages over in vitro cell culture studies. They allow for the study of diseases and interventions in the context of a whole organism, incorporating complex physiological and pathophysiological processes that cannot be recreated in cell cultures. This is particularly valuable in studying diseases like *POLG* disorders that impact multiple organ systems and have systemic effects. Animal models also provide more practical conditions for testing safety and efficacy of potential therapies in a clinical setting. They allow researchers to assess pharmacokinetics and pharmacodynamics, side effects, and long-term impacts of treatments, which are critical for advancing new therapies from the lab to the clinic. However, considering the limitations of animal models in accurately reflecting human disease phenotypes, it is important to interpret results from these studies with caution and use complementary research methods, such as human cell culture studies, organoids, patient-derived iPSCs, and computational models. These tools can help provide additional insights and validation, and together with animal models, they can strengthen our understanding of *POLG* diseases and expedite the development of effective therapies.

In summary, while acknowledging the limitations of animal models, they continue to serve as valuable tools in biomedical research, including *POLG* disease studies. Through an integrated research approach that combines animal models with other experimental models, we can continue to advance our understanding of complex diseases and develop safer and more effective therapies.

AUTHOR CONTRIBUTIONS

Kristina Xiao Liang and Laurence A. Bindoff contributed to the conceptualization. Cecilie Katrin Kristiansen and Kristina Xiao Liang contributed to the methodology. Jessica Furriol contributed to the statistical analysis. Cecilie Katrin Kristiansen, Kristina Xiao Liang, and Anbin Chen contributed to the investigation. Cecilie Katrin Kristiansen, Kristina Xiao Liang, and Laurence A. Bindoff contributed to the writing of the original draft. Cecilie Katrin Kristiansen, Anbin Chen, Gareth John Sullivan, Laurence A. Bindoff, and Kristina Xiao Liang contributed to review and editing. Laurence A. Bindoff, Gareth John Sullivan and Kristina Xiao Liang contributed to funding acquisition. Kristina Xiao Liang, Gareth John Sullivan, and Laurence A. Bindoff contributed to the resources. Kristina Xiao Liang and Laurence A. Bindoff contributed to the supervision. All authors agree to the authorships.

ACKNOWLEDGMENTS

The authors encourage all lab members for discussions and critical reading of the manuscript. We are grateful to the Molecular Imaging Centre, Flow Cytometry Core Facility at the University of Bergen in Norway.

FUNDING INFORMATION

This work was supported by the following funding: K.L. was supported by University of Bergen Meltzers Høyskolefonds (project number: 103517133) and Gerda Meyer Nyquist Guldbrandson og Gerdt Meyer Nyquists legat (project number: 103816102). L.A.B. was supported the Norwegian Research Council (project number: 229652), Rakel og Otto Kr. Bruuns legat and Gerda Meyer Nyquist Guldbrandson og Gerdt Meyer Nyquists legat. G.J.S. was partly supported by the Norwegian Research Council through its Centre of Excellence funding scheme (project number: 262613). We are also grateful to the family of Hallvard Auganes for donations to this research.

DISCLOSURES

The authors declare no competing interests.

DATA AVAILABILITY STATEMENT


The RNA-seq data in this publication have been deposited in NCBI's Gene Expression Omnibus and are accessible through GEO Series accession number GSE227959 (<https://www.ncbi.nlm.nih.gov/geo/query/acc.cgi?acc=GSE227959>). The data that support the findings of this study are available upon request from the corresponding authors.

ORCID

Cecilie Katrin Kristiansen  <https://orcid.org/0000-0002-4217-424X>

Jessica Furriol  <https://orcid.org/0000-0002-8842-534X>

Anbin Chen  <https://orcid.org/0000-0002-0481-7216>

Gareth John Sullivan  <https://orcid.org/0000-0001-8718-7944>

Laurence A. Bindoff  <https://orcid.org/0000-0003-0988-276X>

Kristina Xiao Liang  <https://orcid.org/0000-0002-3586-4218>

REFERENCES

- Graziewicz MA, Longley MJ, Copeland WC. DNA polymerase γ in mitochondrial DNA replication and repair. *Chem Rev*. 2006;106:383-405.
- Copeland WC. Defects in mitochondrial DNA replication and human disease. *Crit Rev Biochem Mol Biol*. 2012;47:64-74.
- Hikmat O, Naess K, Engvall M, et al. Simplifying the clinical classification of polymerase gamma (POLG) disease based on age of onset; studies using a cohort of 155 cases. *J Inherit Metab Dis*. 2020;43:726-736.
- Tzoulis C, Engelsens BA, Telstad W, et al. The spectrum of clinical disease caused by the A467T and W748S POLG mutations: a study of 26 cases. *Brain J Neurol*. 2006;129:1685-1692.
- Hakonen AH, Heiskanen S, Juvonen V, et al. Mitochondrial DNA polymerase W748S mutation: a common cause of autosomal recessive ataxia with ancient European origin. *Am J Hum Genet*. 2005;77:430-441.
- Pfeffer G, Horvath R, Klopstock T, et al. New treatments for mitochondrial disease—no time to drop our standards. *Nat Rev Neurol*. 2013;9:474-481.
- Tzoulis C, Tran GT, Schwarzmüller T, et al. Severe nigrostriatal degeneration without clinical parkinsonism in patients with polymerase gamma mutations. *Brain*. 2013;136:2393-2404.
- Tzoulis C, Tran GT, Coxhead J, et al. Molecular pathogenesis of polymerase γ -related neurodegeneration. *Ann Neurol*. 2014;76:66-81.
- Zhao X, Bhattacharyya A. Human models are needed for studying human neurodevelopmental disorders. *Am J Hum Genet*. 2018;103:829-857.
- Sunitha K, Hemshekhar M, Thushara RM, et al. N-Acetylcysteine amide: a derivative to fulfill the promises of N-Acetylcysteine. *Free Radic Res*. 2013;47:357-367.
- Janssen MCH, Koene S, de Laat P, et al. The KHENERGY study: safety and efficacy of KH176 in mitochondrial m.3243A>G spectrum disorders. *Clin Pharmacol Ther*. 2019;105:101-111.
- Zesiewicz T, Salemi JL, Perlman S, et al. Double-blind, randomized and controlled trial of EPI-743 in Friedreich's ataxia. *Neurodegener Dis Manag*. 2018;8:233-242.
- Lyseng-Williamson KA. Idebenone: a review in Leber's hereditary optic neuropathy. *Drugs*. 2016;76:805-813.
- Fujii T, Nozaki F, Saito K, et al. Efficacy of pyruvate therapy in patients with mitochondrial disease: a semi-quantitative clinical evaluation study. *Mol Genet Metab*. 2014;112:133-138.
- Murayama K, Shimura M, Liu Z, Okazaki Y, Ohtake A. Recent topics: the diagnosis, molecular genesis, and treatment of mitochondrial diseases. *J Hum Genet*. 2019;64:113-125.
- Aldossary AM, Tawfik EA, Alomary MN, et al. Recent advances in mitochondrial diseases: from molecular insights to therapeutic perspectives. *Saudi Pharm J*. 2022;30:1065-1078.

17. Szeto HH. First-in-class cardioprotective compound as a therapeutic agent to restore mitochondrial bioenergetics. *Br J Pharmacol*. 2014;171:2029-2050.
18. Blázquez-Bermejo C, Carreño-Gago L, Molina-Granada D, et al. Increased dNTP pools rescue mtDNA depletion in human POLG-deficient fibroblasts. *FASEB J*. 2019;33:7168-7179.
19. Bulst S, Holinski-Feder E, Payne B, et al. In vitro supplementation with deoxynucleoside monophosphates rescues mitochondrial DNA depletion. *Mol Genet Metab*. 2012;107:95-103.
20. Burgin HJ, Lopez Sanchez MIG, Smith CM, Trounce IA, McKenzie M. Pioglitazone and deoxyribonucleoside combination treatment increases mitochondrial respiratory capacity in m.3243A>G MELAS cybrid cells. *Int J Mol Sci*. 2020;21:2139.
21. Bulst S, Abicht A, Holinski-Feder E, et al. In vitro supplementation with dAMP/dGMP leads to partial restoration of mtDNA levels in mitochondrial depletion syndromes. *Hum Mol Genet*. 2009;18:1590-1599.
22. Domínguez-González C, Madruga-Garrido M, Mavillard F, et al. Deoxynucleoside therapy for thymidine kinase 2-deficient myopathy. *Ann Neurol*. 2019;86:293-303.
23. Disease-specific phenotypes in iPSC-derived neural stem cells with POLG mutations | EMBO Molecular Medicine. Accessed September 14, 2022. <https://www.embopress.org/doi/full/10.15252/emmm.202012146>
24. King MP, Attardi G. Isolation of human cell lines lacking mitochondrial DNA. *Methods Enzymol*. 1996;264:304-313.
25. Leibowitz RD. The effect of ethidium bromide on mitochondrial DNA synthesis and mitochondrial DNA structure in HeLa cells. *J Cell Biol*. 1971;51:116-122.
26. Seidel-Rogol BL, Shadel GS. Modulation of mitochondrial transcription in response to mtDNA depletion and repletion in HeLa cells. *Nucleic Acids Res*. 2002;30:1929-1934.
27. King MP, Attardi G. Human cells lacking mtDNA: repopulation with exogenous mitochondria by complementation. *Science*. 1989;246:500-503.
28. Stewart JD, Schoeler S, Sitarz KS, et al. POLG mutations cause decreased mitochondrial DNA repopulation rates following induced depletion in human fibroblasts. *Biochim Biophys Acta*. 2011;1812:321-325.
29. Davis AF, Clayton DA. In situ localization of mitochondrial DNA replication in intact mammalian cells. *J Cell Biol*. 1996;135:883-893.
30. Druzhyna NM, Wilson GL, LeDoux SP. Mitochondrial DNA repair in aging and disease. *Mech Ageing Dev*. 2008;129:383-390.
31. Moreno-Loshuertos R, Acín-Pérez R, Fernández-Silva P, et al. Differences in reactive oxygen species production explain the phenotypes associated with common mouse mitochondrial DNA variants. *Nat Genet*. 2006;38:1261-1268.
32. Lam C-W, Yeung W-L, Ling T-K, Wong K-C, Law C-Y. Deoxythymidylate kinase, DTYMK, is a novel gene for mitochondrial DNA depletion syndrome. *Clin Chim Acta Int J Clin Chem*. 2019;496:93-99.
33. Bornstein B, Area E, Flanigan KM, et al. Mitochondrial DNA depletion syndrome due to mutations in the RRM2B gene. *Neuromuscul Disord NMD*. 2008;18:453-459.
34. Gandhi VV, Samuels DC. A review comparing deoxyribonucleoside triphosphate (dNTP) concentrations in the mitochondrial and cytoplasmic compartments of normal and transformed cells. *Nucleosides Nucleotides Nucleic Acids*. 2011;30:317-339.
35. Siibak T, Clemente P, Bratic A, et al. A multi-systemic mitochondrial disorder due to a dominant p.Y955H disease variant in DNA polymerase gamma. *Hum Mol Genet*. 2017;26:2515-2525.
36. Dalla Rosa I, Cámara Y, Durigon R, et al. MPV17 loss causes deoxynucleotide insufficiency and slow DNA replication in mitochondria. *PLoS Genet*. 2016;12:e1005779.
37. González-Vioque E, Torres-Torronteras J, Andreu AL, Martí R. Limited dCTP availability accounts for mitochondrial DNA depletion in mitochondrial Neurogastrointestinal Encephalomyopathy (MNGIE). *PLoS Genet*. 2011;7:e1002035.
38. Hong Y, Kristiansen CK, Chen A, et al. POLG genotype influences degree of mitochondrial dysfunction in iPSC derived neural progenitors, but not the parent iPSC or derived glia. *Exp Neurol*. 2023 Jul;365:114429.
39. Silva-Pinheiro P, Pardo-Hernández C, Reyes A, et al. DNA polymerase gamma mutations that impair holoenzyme stability cause catalytic subunit depletion. *Nucleic Acids Res*. 2021;49:5230-5248.

SUPPORTING INFORMATION

Additional supporting information can be found online in the Supporting Information section at the end of this article.

How to cite this article: Kristiansen CK, Furriol J, Chen A, Sullivan GJ, Bindoff LA, Liang KX. Deoxyribonucleoside treatment rescues EtBr-induced mtDNA depletion in iPSC-derived neural stem cells with POLG mutations. *The FASEB Journal*. 2023;37:e23139. doi:[10.1096/fj.202300650RR](https://doi.org/10.1096/fj.202300650RR)